京都大学防災研究所年報 第 56 号 B 平成 25 年 6 月
Annuals of Disas. Prev. Res. Inst., Kyoto Univ., No. 56 B, 2013

A Study on Mechanism of Large-Scale Landslides and the Prediction

Chen-Yu CHEN(1), Masaharu FUJITA and Daizo TSUTSUMI

(1) Dept. of Civil and Earth Resources Engineering, Graduate School of Engineering, Kyoto University

Synopsis

Recent researches indicated that the large-scale landslide induced by rainfalls usually occurred at the end of the rainfall, and the occurring conditions usually were attributed to the high accumulated rainfall. However, the researches which explore the relation of rainfall-runoff and the scale of the large-scale landslide are rare. This study used the integrated Rainfall-Infiltration-Slope stability model to simulate the process of rainfall-runoff and predict the occurring time and the scale of the large-scale landslide. The simulation showed that the runoff had a double peak pattern in weathered granite slopes with steeper bedrock, but ladder recession pattern in volcanic debris slopes. The bedrock locations had influence on the peak timing and decreasing pattern of the runoff. It is expected to have the possibility of the large-scale landslide evaluation if the relation between the runoff and bedrock locations is further studied.

Keywords: large scale landslides, rainfall, runoff, bedrock, simulation, prediction

1. Introduction

Owing to the global climate change, large-scale landslides induced by typhoons and heavy rainfalls have frequently occurred, and the risk of the catastrophe due to the large-scale landslide is becoming much higher. For example, in Taiwan, a large-scale landslide generated sediment more than 2.7×10^7 m^3 in Shiaolin village during Typhoon Morakot in 2009 (Wu et al., 2011), and resulted in 457 people dead. In Japan, many large-scale landslides were induced by Typhoon Talas in 2011, and some of them created the nature dams and derived the secondary disasters (Yamakoshi et al,. 2012).

Generally, the reasons which cause the large-scale landslide and other geological disasters can be broadly divided into two categories: genes and incentives. The genes mean the region's geology, topography and other natural environment conditions; the incentives indicate the typhoons, heavy rainfalls, and earthquakes. Recent researches indicated that the large-scale landslide induced by rainfalls usually occurred in the end of the rainfall, and the occurring conditions normally were attributed to the high ac-cumulated rainfall (Fujita and Tsutsumi, 2008; Dahal, 2012).

To reduce the risk of the large-scale landslide dis-asters, we have to identify the prone areas of the large-scale landslide by topographic and geologic condition, and predict the occurring time and the scale. For example, Chigira (2009) explored the characteristics of the deep-seated landslide susceptibility zones by case studies. Uchida et al. (2011) considered the topographic and geologic characteristics to identify the areas which were prone to deep-catastrophic landslides.

In addition, the large-scale landslide was considered to be associated with the geological structure. In general, the location of the bedrock is

an important factor. That is, the possibility of occurring large-scale landslides will increase if the location of the bedrock is deeper; on the contrary, the possibility will decrease if the bedrock is at shallow position, and thus the scale of the landslide will be limited.

Due to the fact that the investigation of geological structure is usually time-consuming and expensive, therefore, many researchers tried to explore the geological structure by groundwater flow in the past decades (i.e. called hydrogeology). Partly because the rainfall and runoff data are the important indicators for the change of the slope, partly because they are more readily obtained monitoring data, the rainfall and runoff data are most commonly used in monitoring and analysis for the sediment disaster.

For example, Katsuyama et al. (2008) had compared the rainfall-runoff characteristics of catchments underlain by granitic and sedimentary rock, and explored the effect of the forest age. The findings indicated that the forest age had much less influence to the runoff at the sedimentary rock, but the bedrock geology (i.e. granitic and sedimentary rock) had greater influence to the runoff. The research suggested the bedrock geology was the primary factor on determining rainfall-runoff characteristics. Additionally, Onda et al. (2004) continuously monitored and analyzed the rainfall-runoff data in the different geological areas for a long time. They found that the drainage intensity and frequency were significantly lower in the Mesozoic shale watershed than in the granite watershed, and the research suggested the deep-seated landslides may occur more easily in the Mesozoic shale watershed. Onda et al. (2006) also compared the monitoring data of the rainfall-runoff in different watersheds during several rainfall events, and inferred that the runoff in the granite watersheds mainly came from the infiltration of soil, and in the shale watersheds the runoff came from the bedrock flow. However, the researches which discuss the relation of the rainfall-runoff and the scale of the landslide are relatively rare.

This study will explore the change of the rainfall-runoff under different depths of the bedrock by the numerical simulation. Based on the simulation results, this study proposed a preliminary assessment method of identifying the prone areas of large-scale landslides.

2. Method

2.1 The Integrated Rainfall-Infiltration-Slope stability (IRIS) model

The Integrated Rainfall-Infiltration-Slope stability (IRIS) model was developed by Tsutsumi (2008a). The following will elucidate the relative theory.

2.1.1 Infiltration model

The IRIS model adopts the Richard's equation to simulate the infiltration and water flow in the soil.

$$C(\psi)\frac{\partial \psi}{\partial t} = \nabla \cdot \{K(\psi)[\nabla(\psi + z)]\} \quad (1)$$

where C(ψ) is the soil water capacity and $K(\psi)$ is the hydraulic conductivity. The lognormal model proposed by Kosugi (1996) can be used to represent C(ψ) and $K(\psi)$ for unsaturated condition ($\psi < 0$):

$$C(\psi) = \frac{d\theta}{d\psi} = \frac{\theta_s - \theta_r}{\sqrt{2\pi}\sigma(-\psi)} \exp\left\{-\frac{[\ln(\psi/\psi_m)]^2}{2\sigma^2}\right\} \quad (2)$$

$$K(\psi) = K_s\left[Q\left(\frac{\ln(\psi/\psi_m)}{\sigma}\right)\right]^{1/2}\left[Q\left(\frac{\ln(\psi/\psi_m)}{\sigma} + \sigma\right)\right]^2 \quad (3)$$

Where θ_s [m^3/m^3] is the saturated soil water content, θ_r [m^3/m^3] is the residual soil water content, ψ_m [m] is the pressure potential corresponding to the median soil pore radius, σ is a dimensionless parameter related to the width of the pore-size distribution, and K_s [m/s] is the saturated hydraulic conductivity. The function $Q(x)$ represents the residual normal distribution and can be expressed as

$$Q(x) = \int_x^\infty \frac{1}{\sqrt{2\pi}} \exp\left(-\frac{u^2}{2}\right) du \quad (4)$$

For saturated condition ($\psi \geq 0$), value are set at, $K(\psi) = K_s$ and C(ψ) = 0.

The IRIS model uses the 3D finite element method to solve Richard's equation (Istok 1989).

2.1.2 Slope stability analysis model

The result of infiltration analysis which was calculated by the finite element method aforementioned will be used to conduct a slope stability analysis simultaneously. A simplified Janbu method was used to analyze slope stability because this method can be applied to any shape of slip surface. In the simplified Janbu method, a soil layer is divided into vertical slices, and the balance of stresses and slip condition within each slice is assessed. This method is used to calculate the factor of safety F_s, which can be expressed as

$$F_s = \frac{\sum\left[\left\{c_i' l_i \cos a_i + (W_i - u_i l_i \cos a_i)\tan\phi_i'\right\}/m_a\right]}{\sum \tan a_i} \quad (5)$$

$$m_a = \cos^2 a_i \left(1 + \frac{\tan a_i \tan\phi_i'}{F_s}\right) \quad (6)$$

where subscript i indicates the number of vertical slices of soil layer, c_i' and ϕ_i' represent the cohesion and internal friction angle of the soil, W_i is the weight of slice, a_i and l_i represent the angle and length of the slip surface of the slice, and u_i is the water pressure affected on the slip surface.

2.1.3 Determining critical slip surface

Based on previous studies by Kubota & Nakamura (1991) and Yamagami & Ueta (1988), the dynamic programming (DP) method was used to determine the slip surface that provides a minimum factor of safety. The spatial distribution of pore water pressure, calculated through a rainwater infiltration analysis, was used as input data in the slope stability analysis.

2.2 The simulation of landslide cases using IRIS model

To confirm the applicability of this model, two different types of actual landslide cases were simulated as verification. One case was the deep-seated landslide which occurred in volcanic debris slope, and the other was the shallow landslide which occurred in weathered granite slope.

(1) Taketa City

In September 2005, a deep-seated landslide induced by typhoon 0514 occurred in Senokuchi area, Taketa, Oita Prefecture. The soil consists of loam and volcanic debris. Although the maximum rainfall intensity was only 32mm/h, the duration of the rainfall was more than 48 hours, and the accumulated rainfall was about 536mm. The simulation used the actual rainfall from August 1 to September 3 as antecedent rainfall data, and the prime simulation duration was from September 4 to September 6 with 10 minimums as the time-step of the simulation. Table 1 lists the parameters used in the simulation and the results from the simulation are expressed in Fig. 1.

Table 1 Hydraulic characteristics and soil strength of the soil of the slope in Senoguchi, Taketa city

Hydraulic parameters	K_s	θ_s	θ_r	ψ_m	σ
	cm/s	m^3/m^3	m^3/m^3	cm	-
Surface	2.42×10^{-2}	0.646	0.477	-792	0.875
Middle	3.32×10^{-3}	0.595	0.441	-595	1.36
Lower	5.69×10^{-4}	0.682	0.577	-797	1.02

Soil strength	γ	C	φ
	t/m^3	tf/m^2	degree
	1.92	2.0	17

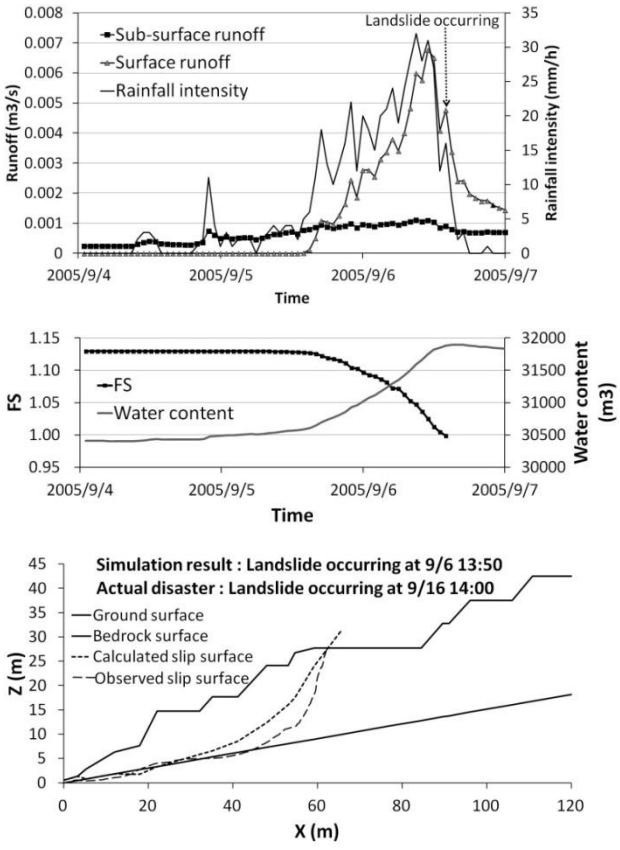

Fig. 1 The simulation of the landslide due to typhoon 0514 in Taketa City

The results show the simulation can calculate not only the change of the safety factor and the scale of the landslide but also the relation of the runoff and the rainfall. In this case, the landslide scale and occurring time of the simulation results are very similar with the actual landslide.

(2) Hofu City

A shallow landslide occurred in Manao, Hofu City, Yamaguchi Prefecture during the heavy rainfall in July 2009. While the accumulated rainfall is not so high (about 332 mm), the higher rainfall intensity (63.5 mm/h) still induced the landslide. The soil thickness of the slope was about 2m and consisted of weathered granite.

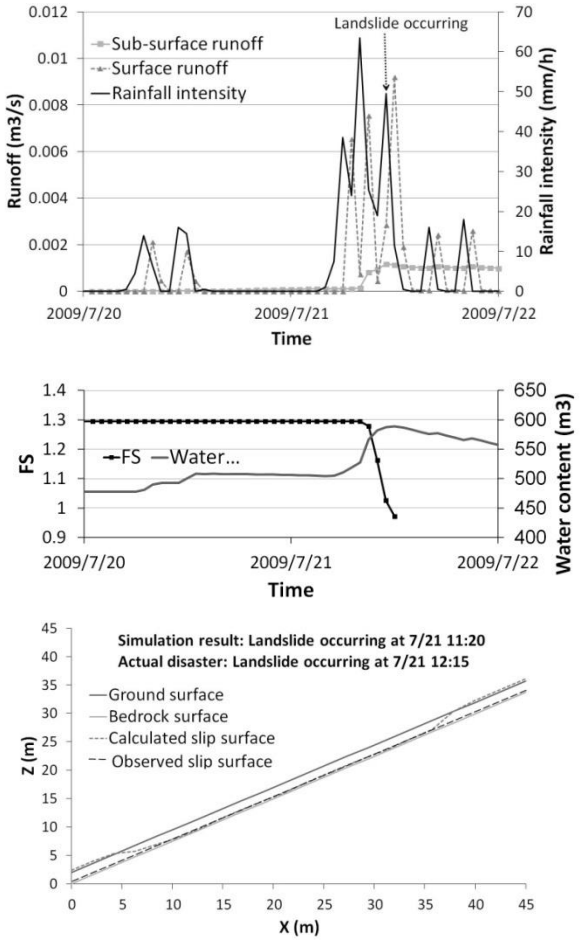

Fig. 2 The simulation of the landslide due to heavy rainfall in Hofu City in 2009

In this case, the simulation adopted the actual rainfall data from June 1 to July 19 as the antecedent rainfall, and the actual rainfall data from July 20 to 21 were applied to simulate. The related parameters were listed in Table 2. Fig. 2 shows the model also can predict the scale and occurring time of the shallow landslide.

Table 2 Hydraulic characteristics and soil strength of the soil of the slope in Manao, Hofu city

Hydraulic parameters	K_s	θ_s	θ_r	ψ_m	σ
	cm/s	m^3/m^3	m^3/m^3	cm	-
	6.71×10^{-3}	0.387	0.128	-91.4	2.269

Soil strength	γ	C	φ
	t/m^3	tf/m^2	degree
	1.92	0.5	33.5

2.3 Simplify the definition of the bedrock location

To explore how the bedrock location had an impact on the occurring time and scale of the landslides, this study simply defined the bedrock location using two parameters: the soil thickness in the downstream (n) and the inclination of the bedrock (β), as shown in Fig. 3.

In order to select the appropriate surface and bedrock slope for subsequent simulation and discussion, this research referred the actual large-scale landslide case occurring in Shiaolin Village in Taiwan in 2009, and adopted 22.85° as the surface slope and 14.0° as the bedrock slope (Tsou et al., 2011). However, due to the horizontal length of this case was up to 1.4 km, this slope size in this study was reduced to 1/10 to reduce the computation efforts, i.e. the following simulation used L = 140 m as the horizontal length, n = 2.7 m as the soil thickness at the downstream, and the width of the slope is 30m.

In additions, this study also adopted two kinds of bedrock inclination, β=8.7° and 19.1°, to compare the difference of the rainfall-runoff between the different bedrock locations. The maximum mesh size of the finite element method in each case of this study was the same. The maximum spacing of the mesh in the x-direction was 5 m, and 1.35 m in the z-direction.

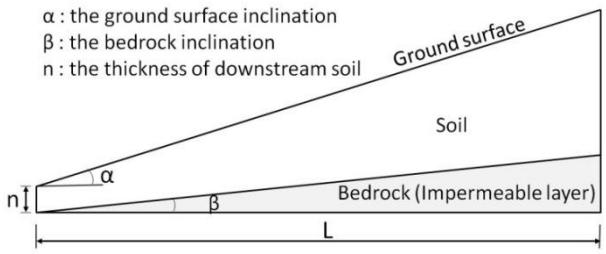

Fig. 3 The simplified bedrock position model

2.4 Parameters for the simulation

Because this study highlights the relation between the bedrock location and the rainfall-runoff, it was assumed that the soil above the bedrock was homogeneous, and the bedrock was impermeable. Besides, this study used two different parameters of hydraulic conductivity and soil strength- one was volcanic debris which had higher water retention, and the other was granite which had higher hydraulic conductivity (Tsutsumi and Fujita, 2008b; Fujita et al., 2010). Table 3 lists the parameters.

Table 3 Hydraulic characteristics and soil strength of the soil of the simplified slope

Hydraulic parameters	K_s	θ_s	θ_r	ψ_m	σ
	cm/s	m^3/m^3	m^3/m^3	cm	-
Weathered granite	6.71×10^{-3}	0.387	0.128	-91.38	2.27
Volcanic debris	3.50×10^{-3}	0.684	0.577	-797.4	2.53

Soil strength	γ	C	φ
	t/m^3	tf/m^2	degree
Weathered granite	1.92	0.5	33.5
Volcanic debris	1.92	2	17

Symbols were used in the study to describe the bedrock geology and inclination. For example, "VB14" represents the soil consisted of volcanic debris and the inclination of bedrock was 14°. "GB8.7" implied the soil consisted of granite, and the inclination of bedrock was 8.7°.

2.5 Methods of setting initial conditions

To simulate the natural soil moisture distribution and eliminate the effect of the different initial water pressure head for the subsequent simulation, the methods of setting initial condition for the water pressure head in this study were described as following:

(1) Two kinds of the different initial water pressure head (ψ= -0.01m and ψ= -0.1m) were given respectively in the soil for two identical slopes.
(2) The two identical slopes which had the different initial water pressure head were continued to drain off the water naturally.
(3) To avoid the soil becoming excessively dry, the two slopes were given a fixed intensity rainfall (0.1 mm/h) during the drainage period.
(4) Continued to drain off the water naturally until the water content and sub-surface flow in the two slopes were same, that is, the soil moisture distributions were identical in the two slopes. Then the study used the soil moisture distribution in the slopes for the formal simulations.

3. Results and discussions

3.1 The influence of bedrock locations on the rainfall-runoff

The rainfall data of simulation was composed of the actual rainfall (September 4-6, 2005, in Taketa City) and no rainfall for 14 days (i.e. totaling 17 days). The time-step of the simulation was 1 min.

3.1.1 Sub-surface runoff response in weathered granite slopes

The three weathered granite slopes with different bedrock locations were used to conduct the rainfall-runoff and slope stability simulation. The safety factors of the slope stability were greater than 1 for all slopes during the period of the simulation, i.e., no collapse occurred in the three slopes.

The rainfall-runoff hydrographs of the weathered granite slopes were shown in Fig. 4. The simulation results of the weathered granite slopes, which had lower water retention but higher hydraulic conductivity, showed that the peak of the sub-surface runoff occurred after the peak of the rainfall, and the peak of the sub-surface runoff occurred later for the deeper bedrock location case. In addition, the discharge of the sub-surface runoff was larger, and the water content of the slope decreased more much in the steeper bedrock case.

After the rainfall, the sub-surface runoff in the weathered granite slopes decreased very quickly, and the rate was slower in the steeper bedrock case. It is worth noting that the runoff of the slopes with

bedrock inclination of 19.1° showed the double peak phenomenon. The distribution of the water pressure head of the slope with bedrock inclination of 14° in each period was shown in Fig. 5.

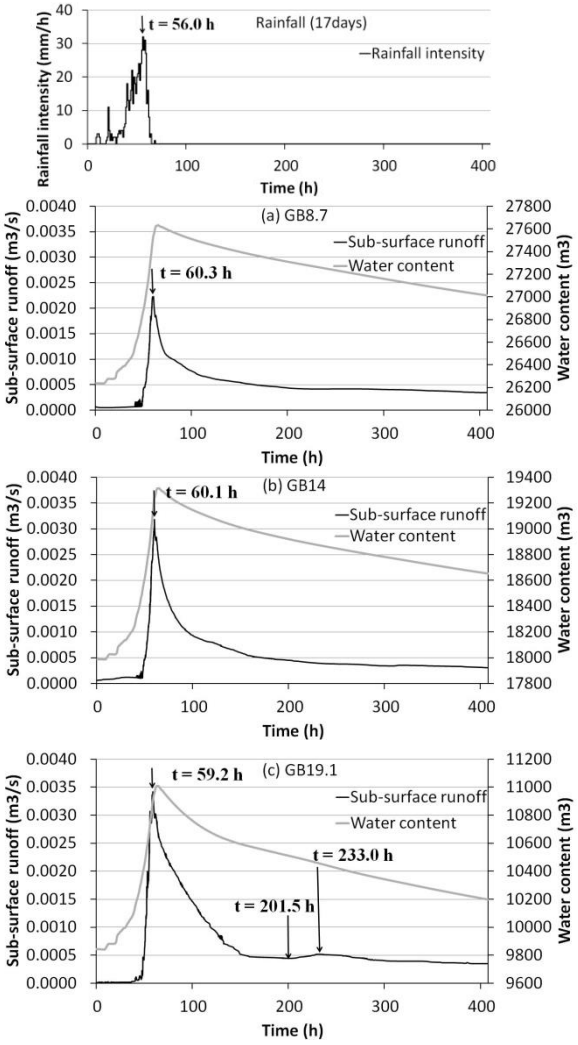

Fig. 4 The rainfall-runoff hydrograph in weathered granite slope (a)bedrock inclination of 8.7° (b)bedrock inclination of 14° (c) bedrock inclination of 19.1°

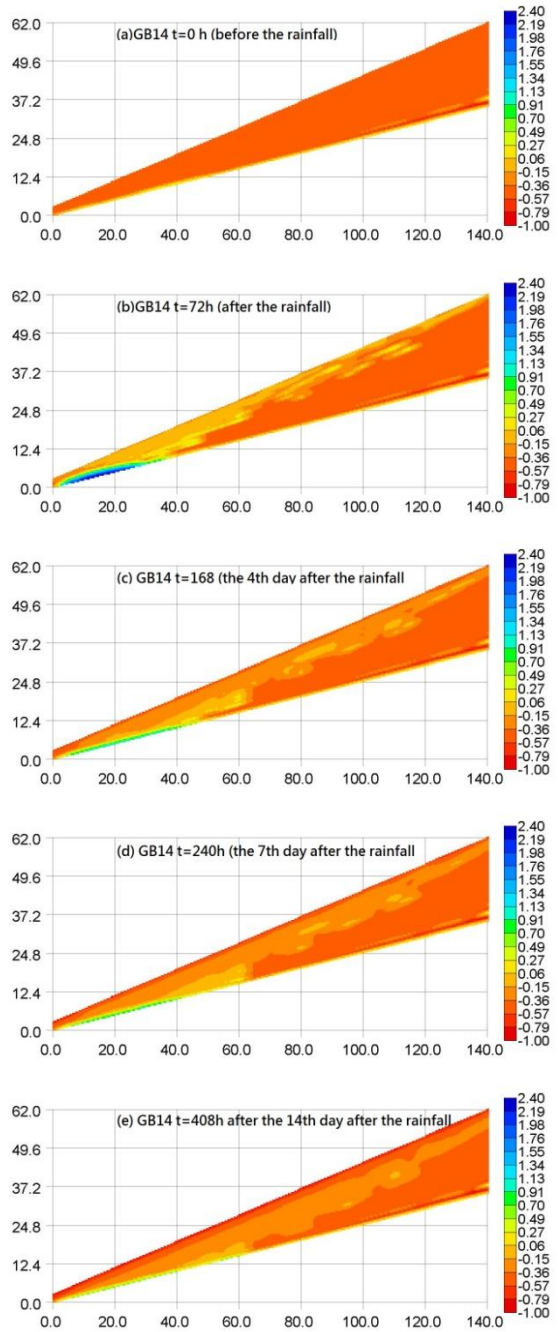

Fig. 5 The water pressure head of the weathered granite slope with bedrock inclination of 14° at various time (a)t=0h (b)t=72h (c)t=168h (d)t=240h (e)t=408h

3.1.2 Sub-surface runoff response in volcanic debris slopes

The three volcanic debris slopes with different bedrock locations were used to conduct the rainfall-runoff and slope stability simulation. The safety factors of the slope stability were greater than 1 for all slopes during the period of the simulation.

The rainfall-runoff hydrographs of the volcanic

debris slope for three different bedrock locations were shown in Fig. 6. The simulation results of the volcanic debris slopes, which had higher water retention and general hydraulic conductivity, showed that the peak and decreasing types of the sub-surface runoff were very different to the weathered granite slopes. The decreasing process of the sub-surface runoff presented ladder recession in volcanic debris slopes, and the discharge of the sub-surface runoff was smaller in the steeper bedrock case. In addition, the occurring time of the peak of the sub-surface runoff for the three bedrock locations was almost the same as the time of the maximum rainfall intensity.

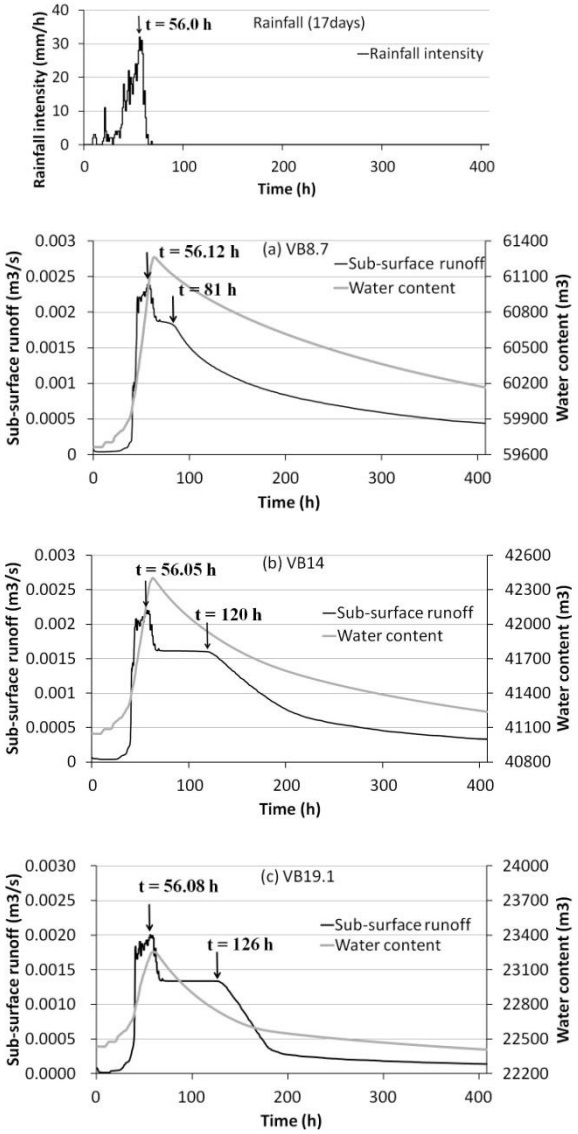

Fig. 6 The rainfall-runoff hydrograph in volcanic debris slope (a)bedrock inclination of 8.7° (b)bedrock inclination of 14° (c) bedrock inclination of 19.1°

The distribution of the water pressure head of the slope with bedrock inclination of 14° in each period was shown in Fig. 7. It is noticed that the volcanic debris slope easily accumulated moisture, and it resulted in unstable slope.

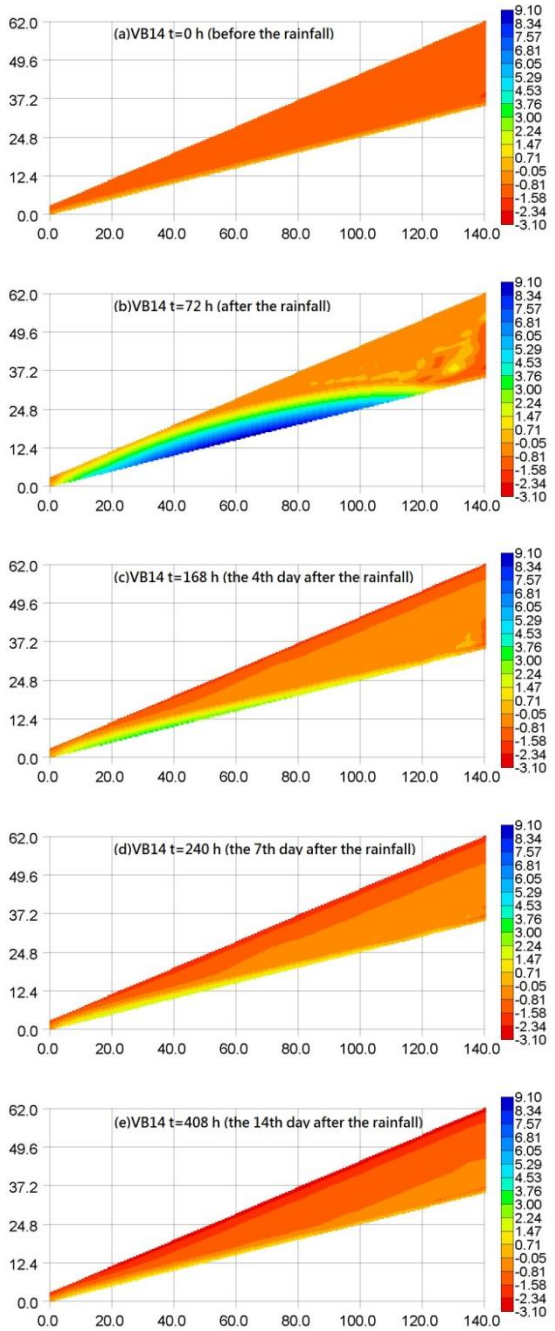

Fig. 7 The water pressure head of the volcanic debris slope with bedrock inclination of 14° at various time (a)t=0h (b)t=72h (c)t=168h (d)t=240h (e)t=408h

3.2 The influence of bedrock locations on the landslide scale and the occurring time

To explore the effect of the different bedrock location condition in the occurring time and scale of the landslide, this study used the constant rainfall intensity (I=20, 40, 60, 80 and 100 mm/h) and duration of 120 hours to conduct simulation. The time-step of the simulation was 1 min, and the simulation results were presented as the following.

3.2.1 Weathered granite slope

For the weathered granite slope cases, the occurring time and the scale of landslides were listed in Table 4, and the critical slip surfaces were shown in Fig. 8.

Due to the higher permeability of weathered granite soil, the water content of the slope can decrease quickly, and the higher water pressure head area usually occurs in the downstream. So regardless of the bedrock locations, the critical slip surfaces in all cases formed in the downstream of the slope during various rainfall intensities, and the scales of landslides were smaller than the volcanic debris slope. In addition, the results in Table 4 also indicated that the landslide occurred earlier when the rainfall intensity was higher. However, due to using the constant rainfall intensity during the simulation, once the surface soil on the slope was saturated; the rainfall can only convert into the surface runoff without infiltration. Therefore, the slip surfaces were identical in the different rainfall intensities sometimes.

Although the initial safety factor of the slope stability was higher for the weathered granite slopes with the steeper bedrock, the landslide occurred earlier. This result could be attributed to the different soil thickness that affected the infiltration time under the higher permeability condition.

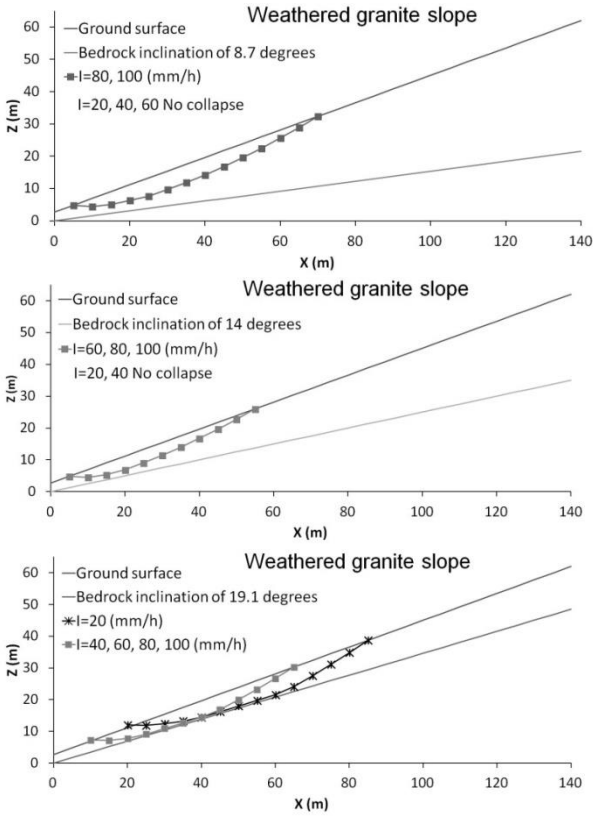

Fig. 8 The critical slip surface of weathered granite slope at different bedrock locations under various rainfall intensities

Table 4 The occurring time and scale of landslides for the weathered granite slope under different rainfall intensities

Bedrock inclination	8.7°		14°		19.1°	
Initial FS	1.568		1.697		1.791	
Rainfall intensity	Time	Scale	Time	Scale	Time	Scale
mm/h	min	m^3/m	min	m^3/m	min	m^3/m
I=20	No collapse		No collapse		5073	265.2
I=40	No collapse		No collapse		3703	176.3
I=60	No collapse		5594	141.5	3321	176.3
I=80	5884	252.9	4478	141.5	2689	176.3
I=100	4966	252.9	3451	141.5	2512	176.3

3.2.2 Volcanic debris slope

For the volcanic debris slope during the different rainfall intensities, the occurring time and the scale of landslides were listed in Table 5, and the critical slip surfaces were shown in Fig. 9.

Since the volcanic debris soil has higher water-retention capacity and relative lower permeability, the higher water pressure head area, which usually caused the slope instability, could occur at the mid- to upstream of the slope, and may

cause the larger-scale landslides. The simulation result also showed that the scale of the landslide was larger in the deeper bedrock location case, and the higher rainfall intensity resulted in the earlier landslide. In addition, the initial safety factor of the slope stability was higher for the steeper bedrock, and the landslide occurred later for the steeper bedrock. The result is different to the weathered granite slopes.

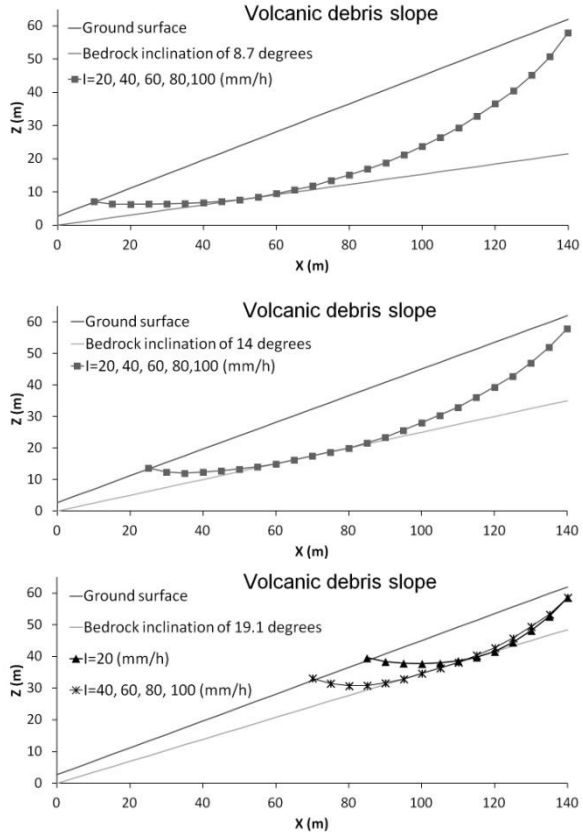

Fig. 9 The critical slip surface of volcanic debris slope with different bedrock locations under various rainfall intensities

Table 5 The occurring time and scale of landslides for the volcanic debris slope under different rainfall intensities

Bedrock inclination	8.7°		14°		19.1°	
Initial FS	1.011		1.076		1.272	
Rainfall intensity	Time	Scale	Time	Scale	Time	Scale
mm/h	min	m^3/m	min	m^3/m	min	m^3/m
I=20	780	1994.1	1496	1429.9	2382	438.0
I=40	428	1994.1	1014	1429.9	1313	581.7
I=60	336	1994.1	754	1429.9	1134	581.7
I=80	279	1994.1	588	1429.9	973	581.7
I=100	239	1994.1	531	1429.9	842	581.7

3.3 Discussions

The simulation result of section 3.1 showed that the weathered granite slopes, which had higher hydraulic conductivity and lower water retention capacity, presented double-peak sub-surface runoff phenomenon in the slope with bedrock inclination of 19.1°. Some studies had revealed the phenomenon of double or delayed hydrograph peak in the actual monitoring cases (Weyman, 1974; Anderson and Burt, 1978; Hihara and Suzuki, 1988), and the phenomenon usually occurred in low relief hillslopes with thick colluvium. Generally, the double peak of the runoff was generated by the hillslope throughflow (Onda, 1992; Onda et al., 2001). However, the simulation results for the volcanic debris slopes, which had lower hydraulic conductivity and higher water retention capacity, showed that the sub-surface runoff didn't appear the double peak phenomenon but the ladder recession of decreasing process.

In spite of the difference of the sub-surface runoff types in the weathered granite and volcanic debris slopes, the simulation results indicated that the influence of bedrock locations was apparent on the discharge and decreasing pattern of the sub-surface runoff. Thus, if we can establish the relation between the rainfall-runoff and the bedrock inclination by continuous and long-term monitoring, it may have the opportunity to develop the simple method of detecting the bedrock location.

Because the volcanic debris soil had high water retention capability, the groundwater table in the volcanic debris slope was obviously higher than the weathered granite slope (see the GB14 of Fig. 5 and VB14 of Fig. 7, all at t = 72hr). It seemed to indicate the volcanic debris slope tends to form a large-scale landslide more likely than the weathered granite slope. This tendency was consistent with the simulation of Fig. 8 and Fig. 9, and Onda et al. (2004) also mentioned of the same results.

Regarding the influence of bedrock locations on the scale of landslides, the simulation results of section 3.2 suggested that for the volcanic debris slopes, which had higher potential of the large-scale landslide, the safety factor of the slope stability was lower and the scale of the landslide was larger in the gentler bedrock. If we can identify the bedrock locations, we could perform preliminary assessment

of the potential of large-scale landslides. The aforementioned proposal of using the rainfall-runoff data to determine the bedrock locations may support this idea.

In addition, the simulation results showed that the influence of bedrock locations on the occurring time of the landslide was different in the weathered granite slopes and the volcanic debris slopes. The findings seemed to indicate that the bedrock location really affected the occurring time of the landslide, but the soil parameters (such as hydraulic characteristics and soil strength) were the key factors for landslides.

4. Conclusion

Compared with other types of sediment disasters, the large-scale landslide had the lower occurrence possibility but the larger scale and extensive disaster. Due to the complex mechanism of the large-scale landslide, the studies of assessing potential and prediction for the large-scale landslide were relative insufficient.

Generally, the depth of the bedrock positions had a certain impact on the potential of large-scale landslides. The traditional investigation of bedrock location was mostly time-consuming and expensive. This study preliminarily explored the relation between the rainfall-runoff and bedrock locations by the Integrated Rainfall-Infiltration-Slope stability (IRIS) model. The proposed relation in this study can be used as a preliminary method to determine the bedrock locations, and as the basis for further potential evaluation of large-scale landslides.

References

Anderson, M. G. and Burt, T. P. (1978): The role of topography in controlling throughflow generation, Earth Surface Processes, Vol.3, No.4, pp.331-344.

Chigira, M. (2009): September 2005 rain-induced catastrophic rockslides on slopes affected by deep-seated gravitational deformations, Kyushu, southern Japan, Engineering Geology, Vol.108, No.1-2, pp.1-15.

Dahal, R. K. (2012): Rainfall-induced landslides in Nepal, International Journal of Erosion Control Engineering, Vol.5, No.1, pp. 1-8.

Fujita, M., Ohshio, S. and Tsutsumi, D. (2010): Effect of climate change on slope failure risk degree in river basin, Annuals of Disas. Prev. Res. Inst., Kyoto Univ., Vol.53B, pp. 515-525.

Fujita, M. and Tsutsumi, D. (2008): Several important issues from field and model investigations on landslides, Proceedings of hydraulic engineering, Vol. 52, pp. 9-12.

Hihara, T. and Suzuki, K. (1988): The double-peaked hydrograph during storm events in a small watershed of the tama hills, west of Tokyo, Geographical Review of Japan, Vol. 61, No. 11, pp. 804-815.

Istok, J. (1989): Groundwater Modeling by the Finite Element Method, Washington DC, American Geophysical Union.

Katsuyama, M., Fukushima, K. and Tokuchi, N. (2008): Comparison of rainfall-runoff characteristics in forested catchments underlain by granitic and sedimentary rock with various forest age, Hydrological Research Letters, Vol. 2, pp. 14-17.

Kosugi, K. I. (1996): Lognormal distribution model for unsaturated soil hydraulic properties, Water Resource Research, Vol. 32, No. 9, pp. 2697-2703.

Kubota, T. and Nakamura, H. (1991): Landslide susceptibility estimation by critical slip surface analysis combined with reliable analysis, Journal of Japan Landslide Society, Vol. 27, No. 4, pp. 18-25.

Onda, Y. (1992): Influence of water storage capacity in the regolith zone on hydrological characteristics, slope processes and slope form, Zeitschrift für Geomorphologie Nene Folge, Vol. 36, pp. 165-178.

Onda, Y., Komatsu, Y., Tsujimura, M. and Fujihara, J. (2001): The role of subsurface runoff through bedrock on storm flow generation, Hydrological Processes, Vol. 15, No. 10, pp. 1693-1706.

Onda, Y., Tsujimura, M., Fujihara, J. and Ito, J.I. (2006): Runoff generation mechanisms in high-relief mountainous watersheds with different underlying geology, Journal of Hydrology, Vol. 331, No. 3-4, pp. 659-673.

Onda, Y., Tsujimura, M. and Tabuchi, H. (2004): The role of subsurface water flow paths on

hillslope hydrological processes, landslides and landform development in steep mountains of Japan, Hydrological Processes, Vol. 18, No. 4, pp. 637-650.
Tsou, C.Y., Feng, Z.Y. and Chigira, M. (2011): Catastrophic landslide induced by Typhoon Morakot, Shiaolin, Taiwan, Geomorphology, Vol. 127, No. 3-4, pp. 166-178.
Tsutsumi, D. and Fujita, M. (2008a): Relative importance of slope material properties and timing of rainfall for the occurrence of landslides, International Journal of Erosion Control Engineering, Vol. 1, No. 2, pp. 79-89.
Tsutsumi, D. and Fujita, M. (2008b): Study on processes of landslide occurrence depending on the soil physical properties, Proceedings of hydraulic engineering, Vol. 52, pp. 565-570.
Uchida, T., Yokoyama, O., Suzuki, R., Tamura, K. and Ishizuka, T. (2011): A new method for assessing deep catastrophic landslide susceptibility, International Journal of Erosion Control Engineering, Vol. 4, No. 2, pp. 32-42.
Weyman, D. (1974): Runoff processes, contributing area and streamflow in a small upland catchment, In: Gregory, K. and Walling, D. (eds.) Fluvial Processes in Instrumented Watersheds. UK: Institute of British Geographers Special Edition No. 6.
Wu, C.H., Chen, S.C. and Chou, H.T. (2011): Geomorphologic characteristics of catastrophic landslides during typhoon Morakot in the Kaoping Watershed, Taiwan, Engineering Geology Vol. 123, No. 1-2, pp. 13-21.
Yamagami, T. and Ueta, Y. (1988): Search for critical slip lines in finite element stress fields by dynamic programming, Proc. 6th International Conference on Numerical Methods in Geomechanics, Innsbruck, Austria.
Yamakoshi, T., Ishizuka, T., Kaji, A., Ito, Y., Osaka, S. and Nakagome, A. (2012): Quick monitoring tool for landslide dam outburst debris flow and its application to the actual disaster, EGU: 6882.

(Received June 11, 2013)